ORIGINAL ARTICLE

Field Experiments to Identify and Eliminate Recirculation Zones to Improve Indoor Ventilation: Comparison with CFD

Krishnendu Sinha[1] · Mani Shankar Yadav[1] · Rajasekharan Jayakrishnan[1] · Guruswamy Kumaraswamy[1] · Janani Srree Murallidharan[1] · Vivek Kumar[2]

Abstract

Ventilation of shared indoor spaces is crucial for mitigating air-borne infection spread among its occupants. Replacing the air in a room with fresh air is key to minimize the concentration of potentially infectious aerosol generated in the room. Recirculating air flow present at corners and around obstacles can trap air and infectious aerosol. This can significantly delay their evacuation by the ventilation system. Knowing the location and extent of such recirculation zones is, therefore, important. In this work, we present flow visualization experiments to identify recirculation zones in an enclosed space. It is based on the deflection of the smoke streak generated by an incense stick. We use particle image velocimetry (PIV) post-processing to quantify the deflection of the smoke streak and use it as an indicator of the direction of local air flow. Positive deflection, defined as the deflection towards the exit location, is associated with primary flow present in well-ventilated regions of the room. On the other hand, negative deflection indicates reversed flow in recirculation zones, where the smoke streak is defined away from the exit location. The technique is applied to a public shared washroom, where the toilet seat is found to be in a well-ventilated region, while the washbasin is in a large recirculation zone. We compare the experimental point measurements with flow field solution obtained using computational fluid dynamics (CFD). We also explore geometry modifications as a strategy to eliminate the recirculation zone over the washbasin.

keywords Ventilation · Infectious aerosol · Flow visualization · Intervention study · Computational fluid dynamics

Introduction

Air-borne transmission of infectious diseases like, COVID-19, pose a major health risk for billions of people across the world. Bio-aerosol generated from an infected person, while breathing, talking, coughing or sneezing can be convected by air flow. This can infect other people in the vicinity, who are exposed to the infectious aerosol for a period of time. Face masks and physical distancing are, therefore, recommended to reduce infection spread. The risk of infection is particularly high in closed spaces, where the aerosol can be trapped in the air inside a room for a long duration, potentially infecting a large number of people. It is, therefore, necessary to have adequate ventilation of shared spaces, like classroom, offices, restaurants and public transport, to name a few.

Ventilation of closed spaces is usually prescribed in terms of the number of air changes per hour (ACH) (Bhagat et al. 2020). This is based on the volume flux of fresh air entering the room and the volume of the room. It is an estimate of the average age of air in the room, and is based on the fully mixed reactor model (Bazant and Bush 2021). It assumes that the infectious aerosol is uniformly distributed in the air contained in the room, and that the air in every part of the room is replaced at the same rate. This estimate can be grossly inadequate, as shown in a recent study (Sinha et al. 2021).

The rate at which air is replaced in a room depends on the air circulation pattern set up between the inlet and outlet ventilation ports (Bhagat et al. 2020). These ports could be part of the air-conditioning system, open doors or windows and exhaust fans. The placement of air purifiers and similar devices are also found to alter the air flow pattern in a room (He et al. 2021). Of particular interest are the recirculation

✉ Krishnendu Sinha
  krish@aero.iitb.ac.in

[1] Indian Institute of Technology Bombay, Mumbai, India

[2] Ansys India Pvt. Ltd., Pune, India

zones formed at the corners of the room and around obstacles like furniture (Narayanan and Yang 2021). The air in such recirculation zones remain trapped for a longer duration than the average residence time given by the volumetric ACH estimate (Sinha et al. 2021). This could lead to higher exposure of person seated in recirculation zones to the infectious particles floating in the air. Knowing the air circulation pattern in a room and identifying the recirculating regions are, therefore, important to mitigate the risk of air-borne infection in indoor spaces.

Computational fluid dynamics (CFD) is routinely used to study air flow patterns, identify recirculation zones and devise strategies to improve ventilation of indoor spaces (Wang et al. 2014, 2021; Komperda et al. 2021). However, computer models often come with simplifications of the geometric complexities and assumptions in boundary conditions. These approximations are usually acceptable for proof-of-concept studies or to investigate the underlying flow phenomena. However, experimental validation is essential to substantiate CFD solution. This could be in the form of measuring air flow velocity (Li et al. 2021; Yin et al. 2011), flow visualization (Verma et al. 2020), droplet/contaminant distribution (Yin et al. 2011; Zhang et al. 2021) and CO_2 concentration (Bolashikov et al. 2012; Singer et al. 2021). The majority of such measurements are done in sub-scale laboratory experiments (Eames et al. 2009) or in a mock up (Li et al. 2021); a few exceptions are available in literature (Zhang et al. 2021). However, due to the urgent need to implement retrofit solutions to mitigate infection spread, it is imperative that the designs are tested and verified in a real situation. Field experiments that can be done in a time and cost effective manner are especially important.

In this paper, we present a smoke-based flow visualization technique to identify recirculation regions in a room, and distinguish them from the well-ventilated part of the room. Flow visualization is routinely used in laboratory experiments, where smoke is used to visualize streak lines in a flow (Yang 2001). Smoke visualization has also been used in field studies, where a puff of smoke is injected at a point of interest and its trajectory is tracked in real time; see, for example, the study in a nuclear facility (Strons et al. 2016). In another example from a health care facility, smoke is used as a surrogate to aerosol breathed out by a patient to ascertain the effectiveness of the air flow vents in the room (Cho et al. 2019). Smoke visualization using laser sheet is also used in ventilation studies to assess the overall air flow pattern in a room (Hviid and Petersen 2016).

We use smoke from incense stick as a point measurement of the direction of the local air flow velocity. It is based on the deflection of a smoke streak in the direction of the air velocity. Air flow towards an exit port is considered favorable for evacuating infectious aerosol, and is termed as primary flow in well-ventilated parts of the room. On the other hand, air flow in a direction away from the exit location indicates reversed flow, usually present in recirculation zones. We present a quantitative analysis of the smoke visualization images using particle image velocimetry (PIV) post-processing and arrive at time-averaged deflection angle of the smoke streak. Deflections towards the exit port are taken as positive and vice versa. Thus, differentiating between locations that have positive and negative deflection of the smoke streak allows us to experimentally identify the recirculation zones in the room. This is the primary objective of the current work.

The experiments are complemented with CFD simulation of air flow in an identical configuration. Both qualitative and quantitative comparison are made, where the direction of the computed velocity vector is compared with the smoke deflection angle. It is shown that the experimental values are comparable to the CFD predictions for the configuration tested in this work. We note that incense sticks are widely available in India and neighboring countries, and incense smoke is often used for a quick assessment of air flow. However, to the best of our knowledge, there is no systematic study of this technique, especially with in situ CFD simulations.

The smoke deflection technique can also be used to evaluate potential retrofit solutions to improve ventilation in a room. In the current context, we explore ways to eliminate recirculation zones by directing incoming fresh air into such regions. Here again, we use the incense smoke experiments to evaluate the effectiveness of such retrofit measures. It is shown that reorienting existing doors and windows, or diverting air using louvers can be an effective way to eliminate or alter the recirculation zones in a room.

The paper is organized as follows. The geometry of the indoor space considered in this work and representative air flow pattern are presented in the next section. This is used to identify potential recirculation regions in the room. Next, we describe the experimental methodology, along with the procedure to post-process the smoke visualization videos. This is followed by experimental results obtained at frequently used locations in the room. CFD solution is presented next, along with a detailed analysis of the three-dimensional velocity field, followed by comparison with the experimental data. Discussion of the results and pointers to future work are in the penultimate section. Conclusions are presented in the final section.

Geometry and Airflow Pattern

We consider a typical single-person washroom geometry, as shown in Fig. 1; it has a washbasin next to the door and a toilet seat located in the center of the washroom. Such washrooms are used by multiple people, one after another,
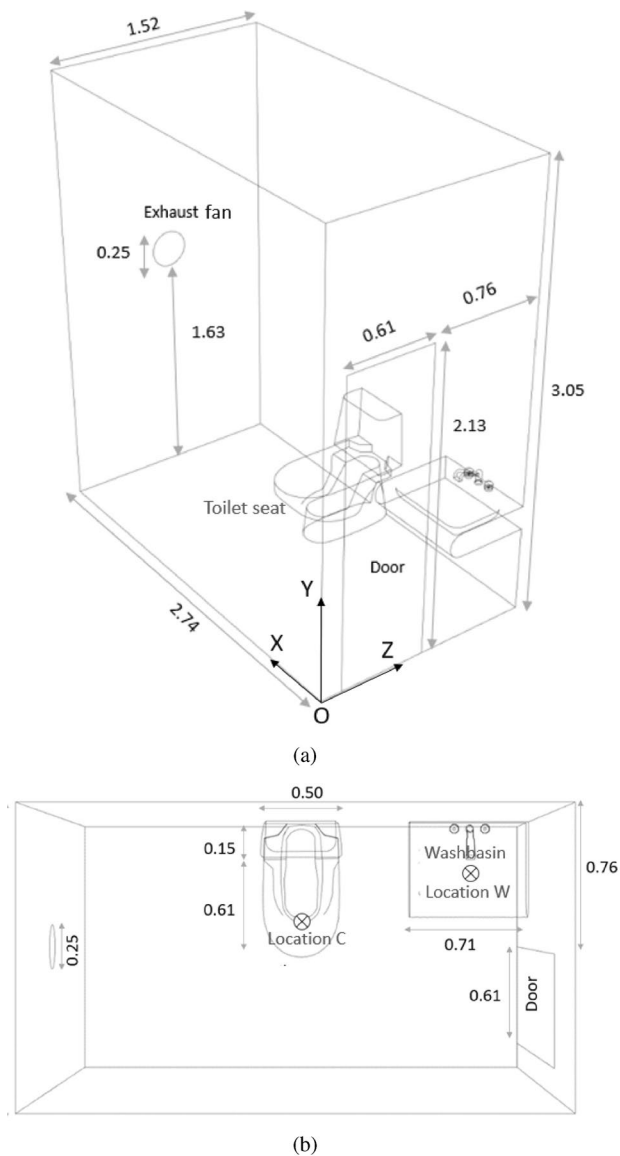
(a)

Fig. 1 A typical shared washroom with a door, an exhaust fan, a toilet seat and a washbasin. **a** Isometric view and **b** top view. All dimensions are in meters, and two frequently used locations (washbasin and toilet seat) are identified by $\otimes$ for conducting smoke deflection experiment. Adapted from Sinha et al. (2021)

and can be commonly found in offices, restaurants and airports. To minimize air-borne infection in this shared space, it is recommended that the air in the washroom is refreshed after every use. This is commonly achieved by an exhaust fan that vents the air out of the washroom. The washroom door is kept open between two consecutive usages, and it acts as an inlet for fresh air. The washroom door opens inside. The washroom also has windows with louvers opening into a common duct; the louvers are closed and there is negligible air leaking through them. The volume flow rate of a typical exhaust fan is 270 m^3/h, or 158.8 cubic feet per
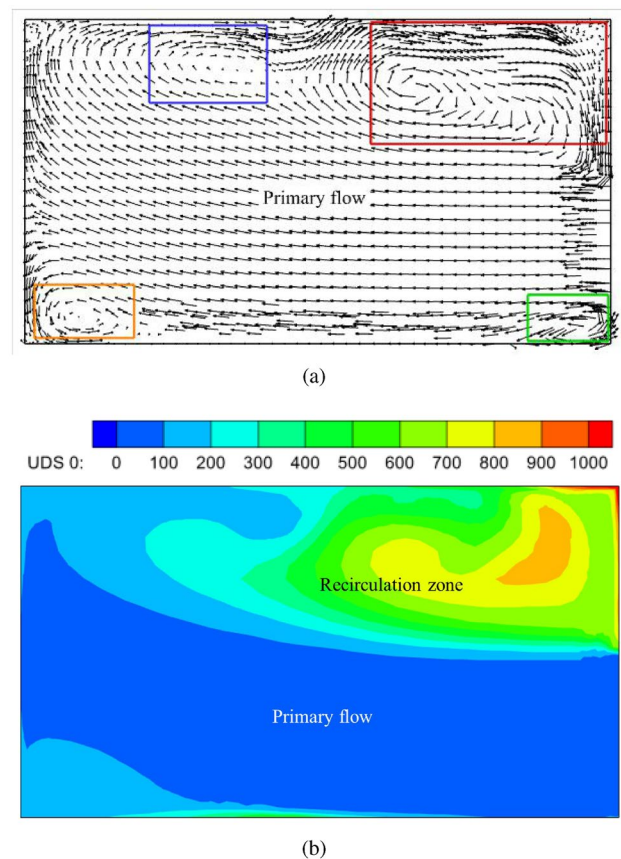

Fig. 2 The computed flow pattern in a horizontal plane at $y = 1$ m showing regions of primary flow and recirculation zones marked by rectangular boxes: **a** velocity vectors **b** flow residence time (s). Adapted from Sinha et al. (2021)

minute (CFM), and it translates to an axial velocity of 1.5 m/s for a fan diameter of 0.25 m (assuming uniform axial flow through the fan).

CFD simulations of this geometry are presented in a recent work (Sinha et al. 2021), and a snapshot of the results are shown in Fig. 2. Velocity vector field in the horizontal plane at $y = 1$ m is used to visualize the air flow pattern. A primary flow is set up between door entry at the right and fan exit location on the left. There is recirculating flow at corners and around obstacles, and they are identified by rectangular boxes. A large recirculation zone is present next to the door over the washbasin (red box in the figure). This is of primary concern as the washbasin is a frequently used location in the washroom. Heavy usage of water in the washbasin can also be a source of droplets and aerosol. The larger droplets tend to settle on surfaces, which can then be sanitized by spray disinfection. On the other hand, small droplets and aerosol can persist in the air trapped in the recirculating flow, potentially exposing subsequent users of the same space (Sinha et al. 2021).

The details of the CFD simulations are presented in the previous work (Sinha et al. 2021). In short, the Reynolds-averaged Navier–Stokes equations are solved for the air flow in the washroom to obtain the three-dimensional steady-state solution. Turbulence is modeled using realizable $k - \epsilon$ model (Shih et al. 1995) with enhanced wall treatment. The simulations are performed using ANSYS Fluent software (ANSYS 2020) and the details of the computational grid and boundary conditions, along with additional plots of the velocity field are given in the original paper (Sinha et al. 2021). Only relevant results are discussed to motivate the experimental work, and decide the locations for conducting smoke visualization studies.

An important aspect of ventilation is the residence time of air at a given point in the room. It is plotted in Fig. 2b, and the procedure to compute it is described in our earlier paper (Sinha et al. 2021). The residence time is an estimate of how long it takes for fresh air entering the room to reach a particular location. Low residence time is representative of well-ventilated parts of the washroom. This corresponds to the primary flow region between the door and the exhaust fan, where the residence time is equal to or less than 50 s. The primary flow covers a part of the toilet seat, which can be a major source of droplets and aerosol (Li et al. 2020; Wang et al. 2020) The primary flow time scale ($\simeq 50$ s) is calculated based on the length of the washroom, i.e. 2.74 m and the velocity (5.8 cm/s) calculated at the door (area 1.3 m^2) using volume flow rate in the domain 270 m^3/h (driven by the exhaust fan). On the other hand, high values of residence time is obtained in the recirculation regions covering the majority of the upper half in the figure. This consists of the washbasin recirculation zone and the small recirculation region next to the toilet seat (blue box in Fig. 2a). The fluid residence time varies between 200 and 800 s in this area, and an average value of 500 s is taken as a representative fluid time scale for the recirculation zone.

The significance of the fluid residence time can be understood by studying the ventilation of droplets and infectious particles from the washroom. Discrete particle tracking simulations (Sinha et al. 2021) show that particles injected in the recirculation region take much longer to evacuate than those injected in the primary flow, for example, at the toilet seat. The fraction of particles remaining in the washroom follows an exponential decay in time, with the characteristic time scale given by the air residence time corresponding to the injection location. Thus, the time scale of ventilation is about ten times higher for the washbasin (recirculation zone time scale of 500 s) than the toilet seat (primary flow residence time of 50 s). It takes about 800 s to evacuate 77% of the particles injected at the washbasin recirculation zone, compared to 100 s for those generated at the toilet seat (Sinha et al. 2021). This gives an estimate of the duration

for which the washroom may be left open between two consecutive usages.

Experimental Setup

The experimental setup for flow visualization using incense smoke is shown in Fig. 3, where typical dimensions are marked. An incense stick is placed at a point of interest, and the smoke emanating from its tip is recorded by a camera (a cell phone camera, in this case). Illumination is provided by a light source, and a dark background is used for better contrast in the images and videos. The tip of an incense stick is 2.5 mm thick and it is typically 5–9 inches long; it poses minimal obstruction to the air flow. We also ensure that the placement of the camera, light source and the dark background sheet does not obstruct or alter the air flow in any way. They are aligned in a direction perpendicular to the local air flow, and the incense stick is placed in between them. We maintain enough gap around the incense stick (typical dimensions mentioned in the figure) for the air flow. Further, it was found that small changes in the location of the camera and the light source did not have any significant effect on the smoke streak deflection.

The smoke from an incense stick in stagnant air rises vertically up due to buoyancy. In the presence of horizontal air flow, the smoke streak is deflected in the direction of the local air velocity. We define the direction towards
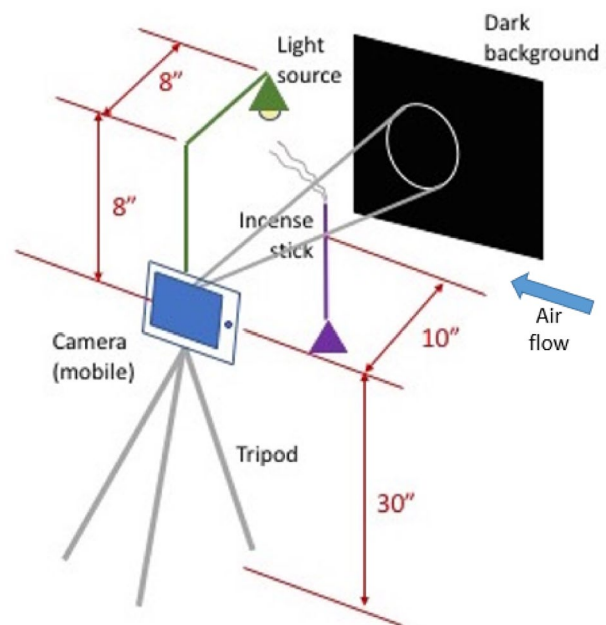
Fig. 3 Schematic of the experimental set up for flow visualization using smoke generated by an incense stick. Typical dimensions of the experimental equipment are shown for reference

the exit location as positive deflection. This is expected to be the case in well-ventilated (primary flow) regions of the room, where the air from such locations directly goes out through the exhaust fan. By comparison, reversed flow in the direction opposite to the exit location is taken to be negative deflection, and is an indicator of recirculating flow. The camera is aligned perpendicular to the local flow direction, such that it captures the horizontal drift of the smoke streak accurately, while minimizing cross-flow effect. We were able to optimize the placement of the camera with some trial and error to ensure good imaging.

Two frequently used locations are considered in the washroom, namely, the washbasin next to the door and the toilet seat at the center of the washroom. A user is expected to spend considerable time at these locations, and thus can potentially be exposed to infectious aerosol present in there. As noted earlier, CFD predicts a large recirculation zone over the washbasin, while the majority of the toilet seat is in the primary flow. We measure the air flow direction at the two locations, marked as C and W in Fig. 1, using the smoke deflection technique and cross-check with the CFD results. We also do a quantitative comparison of the deflection angle obtained from flow visualization with that from CFD simulation.

The smoke streak from an incense stick is inherently unsteady. It is also influenced by the unsteady and turbulent fluctuations in the air flow. We use the following procedure to obtain an estimate of the direction of the local mean velocity of air. First, the flow visualization is recorded at 30 frames per second for about 30 s, giving up to 900 instantaneous images from each experiment. The flow images are analyzed using particle image velocimetry toolbox in Matlab software (MathWorks Inc. 2021). Consecutive images are compared to obtain velocity vectors at points that are uniformly distributed in the field of view. We time-average the instantaneous velocity field, and obtain the deflection angle of the velocity vectors with respect to the vertical direction. The data are in the form of a spatial distribution of the time-averaged deflection angle over an array of points spanning the experimental field of view. The probability distribution function of the deflection angle is then computed, which yields the mean deflection angle and its variance over the experimental window.

We use the 12 MP rear camera of iPhone 7 cell phone, with 4K (2160 pixel) video up to 30 fps. A commonly available cell phone flashlight (iPhone 7 Quad-LED True Tone Flash light in this case) is used as the light source for the experiment, to make it easy to implement anywhere, even without specialized PIV equipment. The smoke visualization is recorded over a rectangular window of 5–13 cm each side; the exact size is reported for each experiment in "Results". The mean deflection angle over this field is representative of the mean air flow velocity spatially averaged over this region. The field of view is small compared to the overall size of the room shown in Fig. 1. The mean deflection angle can thus be taken as a local measurement of the airflow direction at a given point. We also present a convergence study by plotting the sensitivity of the mean and variance values to the number of images used in the PIV analysis.

The location of the tip of the incense stick is mentioned in Table 1, where the uncertainty in the values are also listed. The uncertainty in the x and z coordinates are based on the size of the base support of the incense stick. The vertical height variation is estimated by the length of the incense stick, which varied between 5 and 9 inches between different experimental runs.

Results

The flow visualization experiments and the PIV processed data are presented for the two frequently used locations in the washroom, namely, the toilet seat and the washbasin. Both the open door and the partially closed door configurations are considered.

Primary Flow

The first experiment was conducted by placing the incense stick on top of the toilet seat at the center of the washroom, marked as location C in Fig. 1b. The point is in primary flow, and is expected to be well ventilated by the exhaust fan. Figure 4a shows an instantaneous image of the smoke streak from the incense stick. The smoke is illuminated by a light source which is focused on the tip of the incense stick. The range of illumination, along with the field of view of the camera, determines the length of the smoke streak visible in the experiment. Too large field of view usually results in reduced contrast between the smoke streak and the background illumination. On the other hand, if we use too small window, the smoke streak may oscillate and go out of the field of view for part of the experiment. The full 30 s video is available in multimedia view, where we can see the unsteady oscillations of the smoke streak. These are caused by a combination of air turbulence and inherent instability of smoke streaks. The smoke visualization videos are recorded after the initial transient (20–30 s) has passed. Several runs

Table 1 Location of the tip of the incense stick in the flow visualization experiments

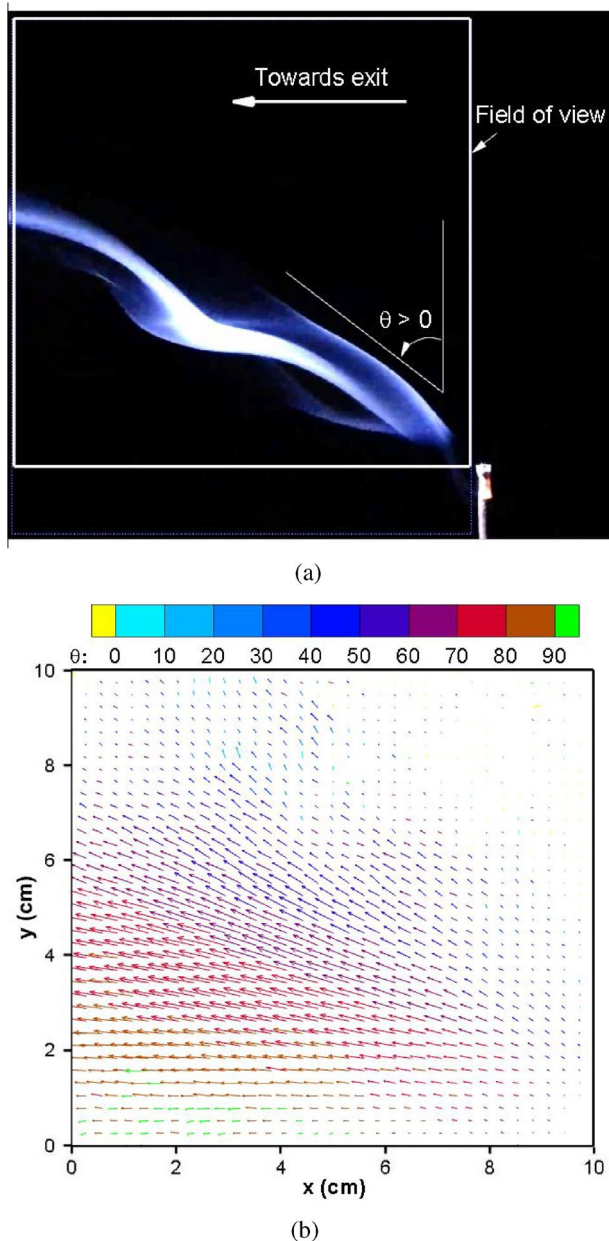| Coordinates	Location C	Location W
x (in m)	1.38 ± 0.03	0.35 ± 0.03
y (in m)	0.61 ± 0.05	1.12 ± 0.05
z (in m)	0.92 ± 0.03	1.27 ± 0.03

(a)

(b)

Fig. 4 Smoke streak deflection experiment at the center of the washroom, location *C* in Fig. 1, with door fully open. **a** Smoke streak deflected towards exhaust fan, and **b** time-averaged velocity vector field obtained using PIV processing (multimedia view)

(30 s each) were conducted and qualitatively similar visualization was obtained in each run. The data from a single run are reported in detail.

Figure 4b plots the time-averaged velocity vectors, computed from 800 instantaneous velocity fields, and the vectors are colored as per their deflection angle. Reliable velocity vectors are obtained in the region covered by the illuminated smoke and its unsteady undulations. Small magnitude vectors outside the illuminated region are possibly

due to background noise; they could be erroneous and are filtered out during the PIV post-processing of the images. We implement a velocity filter such that vectors with magnitude below a cut-off are eliminated. Typically, this cut-off is about 20% of the maximum velocity and is characteristic of the background noise. Additional manual filtering is employed to eliminate a few erroneous vectors, particularly those pointing in the direction opposite to the smoke streak. The manual filtering is usually limited to 1–2 vectors for each experiment.

We observe that the velocity vectors at the upper edge of the smoke streak are deflected by about 45°, while the lower part of the smoke streak shows close to 90° deflection from the vertical direction. Both the velocity vectors and the smoke streak show a deflection due to the air flow velocity towards the left. In the current orientation, this corresponds to the direction towards the exhaust fan, and is defined as positive deflection in the figure. In addition, local variations of velocity vectors and their inclination angle are eliminated by the averaging procedure. The resulting velocity field represent the time-averaged smoke streak deflection caused by the mean air flow velocity at this point. This forms the basis for comparison with steady-state RANS solution of the air flow presented in "Comparison with CFD".

The objective of the smoke visualization experiments is to obtain a single average value of the deflection angle for a given location of the incense stick. This would be representative of the local direction of the steady state air flow velocity. In this respect, the current experiments are aimed towards point measurement at a specific location in space. The quantitative data can thus be compared with CFD. In contrast, the majority of smoke flow visualization experiments in literature provide a qualitative picture of the flow field. They study flow structures, like vortices, and their development in a spatial domain over a finite time duration.

To obtain a single average value of the smoke streak deflection at the center of the washroom, we first plot the probability density function (PDF) of the deflection angle (see Fig. 5). It is in the form of a histogram with 15° intervals, and represents the fraction of points in Fig. 4b that have deflection value in a chosen interval. The data are normalized such that integrating the PDF gives the mean value of the deflection angle. The majority of the velocity vectors have deflection between 45° and 90°, and the PDF tapers off on either sides of this range. There are a small number of vectors with deflection angles less than 0° (deflection opposite to the primary flow) or more than 180° (deflected downward). These are filtered out of the analysis, as described above.

Figure 5a shows the effect of PIV interrogation window on the PDF of the deflection angle. The numbers represent the four passes in PIV processing (from larger to smaller window size) to arrive at the final velocity vector field. There
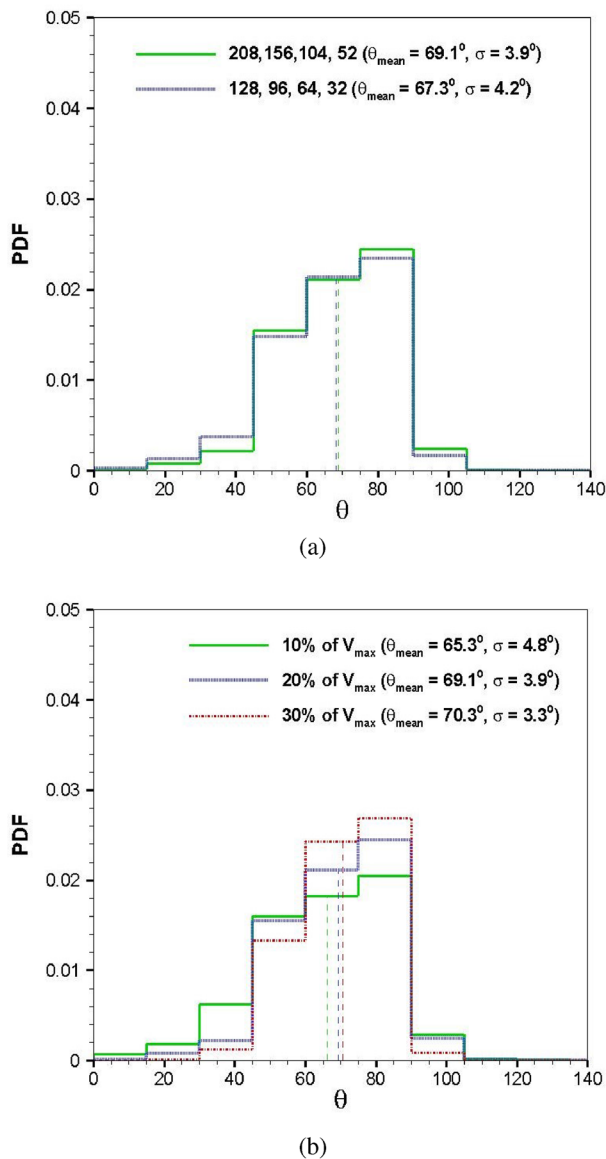
Fig. 5 The probability density function (PDF) of the time-averaged deflection angle of the smoke streak for location C, and its variation with **a** PIV interrogation window and **b** magnitude of velocity filter

is minimal difference in the PDFs obtained using the interrogation windows of (208, 156, 104, 52) vs. (128, 96, 64, 32). The values of θ_{mean} and σ are within 1.8° and 0.3° respectively. We recommend the results obtained using the higher interrogation window for better accuracy. This corresponds to (2.3, 1.7, 1.1, 0.6) cm in physical dimensions. Note that the PDF in Fig. 5a is computed using a velocity filter of 20%. That is, velocity vectors with magnitude less than 20% of the maximum velocity are filtered out. This eliminates the erroneous data at the edge of the smoke streaks, where the resolution may not be adequate. Figure 5b shows that using a higher (30%) and lower (10%) velocity filter gives

qualitatively similar PDFs of the deflection angle. Higher peaks are obtained using higher cut-off value, as expected, and θ_{mean} is found to increase, while σ shows a monotonic decrease with increasing velocity filter value.

We use the PDF corresponding to the higher interrogation window and a 20% velocity filter to obtain $\theta_{mean} = 69.1°$ and $\sigma = 3.9°$ respectively. Positive θ_{mean} indicates that the local flow of air is towards the exit location. We consider the location to be well-ventilated, where any infectious aerosol generated at this point will be evacuated efficiently by the air flow. The PDF also shows that more than 90% of the velocity vectors are deflected in the range of 45° to 90°, which means that the smoke streak is almost always deflected towards the exhaust fan by more than 45°. In spite of the unsteady turbulent fluctuations of the smoke, it is almost always carried towards the exhaust fan, and the same can be expected to be true for any infectious particles generated at the toilet location. This can be qualitatively seen in the video of the smoke visualization, and the PDF of the deflection angle quantifies the effect.

Reversed Flow

We next place an incense stick at the location W marked in the washbasin (see Fig. 1b) and follow the same procedure of experiment and PIV post-processing as described above. The field of view in this case is 5.5 cm × 6 cm. The results are presented in Figs. 6 and 7.

The main difference is in the deflection of the smoke streak to the right (away from the exit), instead of to the left (towards the exit) in the primary flow. Both the instantaneous velocity field in Fig. 6a and the time-averaged velocity vectors in Fig. 6b show this clearly. Once again, small velocity vectors obtained outside the smoke region are filtered out to obtain a PDF of the deflection angle. Figure 7a shows the PDFs obtained for two sets of PIV interrogation windows, for three different values of the velocity filter. All the PDFs are qualitatively similar to each other, and they show the same trend as described above ("Reversed Flow"). Specifically, there is little variation due to changing interrogation windows from (248, 186, 124, 62) to (128, 96, 64, 32) for a given velocity filter. On the other hand, increasing (decreasing) the value of the velocity cut-off increases (decreases) the peak value of the PDF, while reducing (increasing) the spread of the deflection angle.

As earlier, we recommend the PDF corresponding to the higher interrogation window, corresponding to (3.0, 2.2, 1.5, 0.7) cm in physical dimensions, and a velocity filter of 20% of the maximum velocity magnitude. The mean and standard deviation of the deflection angle are thus obtained as $-57.1°$ and 4.8°, respectively. The majority (91%) of the velocity vectors have deflection angle between $-30°$ and $-90°$. Negative deflection is indicative of reversed flow, as per the
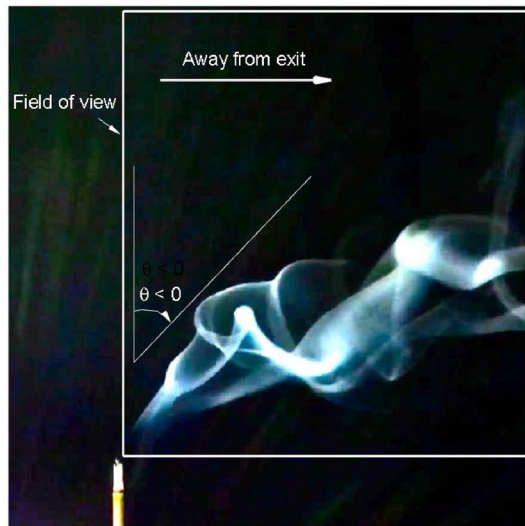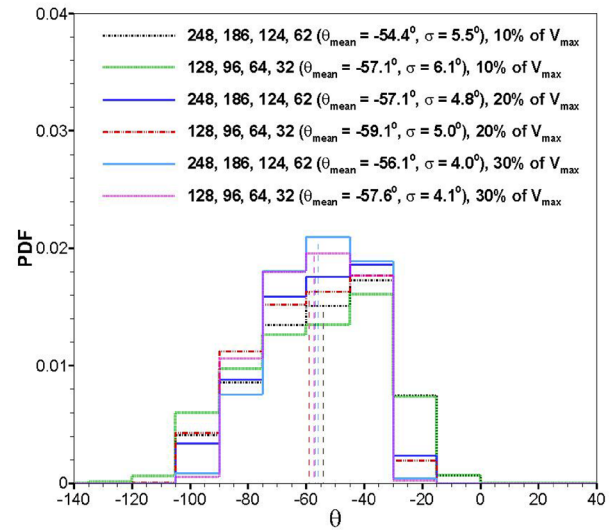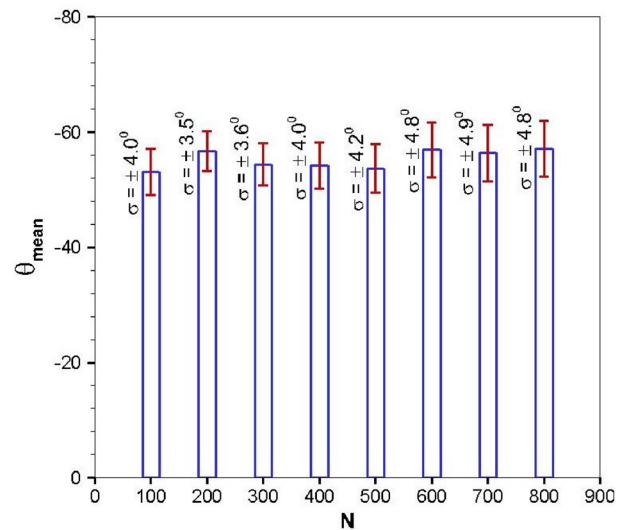
(a)
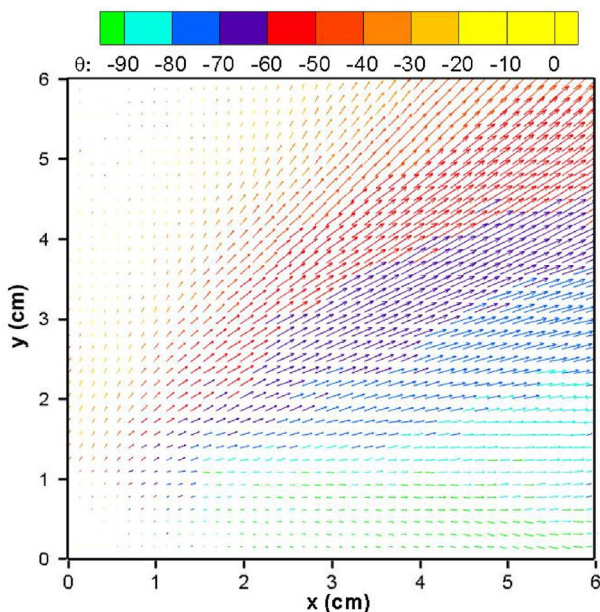
(b)

Fig. 6 Smoke streak deflection experiment at the washbasin, location W in Fig. 1, with door fully open. **a** Smoke streak deflected away from the exhaust fan, and **b** time-averaged velocity vector field obtained using PIV processing (multimedia view)

(a)

(b)

Fig. 7 Variation of the time-averaged deflection angle of the smoke streak at the washbasin location W in terms of **a** the probability density function and **b** time convergence history

current convention. CFD solution in Fig. 2a shows that the washbasin is covered by a large region of recirculating flow, with reversed flow present over the majority of the washbasin. Deflection of the smoke streak away from the direction of the exit can be interpreted as a sign of recirculating air flow, which tend to harbor infectious particles for much longer duration than primary flow. Negative deflection may also mean that the air from this point takes a circuitous route to reach the exit port (see "Location W with Open Door").

This is also undesirable, as infectious particles carried by the flow can thus reach different locations in the room, where they can linger for an extended period.

Figure 7b shows the mean and variance of the time-averaged deflection angle, computed using different number of instantaneous images. We see a systematic convergence of the mean and standard deviation of the deflection angle as the number of images is increased. This also corresponds to a successive increase in the duration of smoke visualization data. For example, 300 images represents the first 10 s of the flow visualization experiment, while 600 images span 20 s of the video. The data shows that the results do not change substantially beyond 600 images; variation in θ_{mean} and σ

Fig. 8 Smoke streak deflection experiment at the washbasin, location W in Fig. 1, with door partially closed at 15°. **a** smoke streak deflected towards the exit location (Multimedia view); **b** time-averaged velocity vector field obtained using PIV processing; **c** probability distribution of the deflection angle obtained using different bin sizes

are within 0.5° and 0.1°, respectively. This indicates that the duration of experiment is long enough and that we have reached statistical convergence. Similar results are obtained for the primary flow location presented in "Primary Flow", where the corresponding variation in the mean and standard deviation beyond 600 images are 0.2° and 0.3°, respectively. We thus recommend that the experiments are conducted for 20 s or more after the initial transient has passed.

Partially Closed Door

We next study the effect of geometric variation in the washroom, in the form of a partially closed door. The objective is to eliminate the recirculation zone formed over the washbasin, thereby facilitating the evacuation of trapped infections particles by the ventilation air flow. It will be shown that changes in the air flow direction at the inlet and outlet ports can make a significant change in the air flow pattern in the room. Here, we orient the door at 15°, as opposed to 90° for the fully open door considered earlier. In the current configuration, orienting the door at 15° directs the incoming air flow towards the washbasin corner located next to the door. This can be used as a strategy to replace the trapped air in the recirculation flow in this region. This can potentially disrupt the recirculation zone, thereby reducing it in size or even eliminate it completely. Similar effects can also be achieved by placing additional fans over the washbasin or by having louvers to direct air into the recirculating zone.

Figure 8a shows the smoke flow visualization (field of view : 11.5 cm × 13 cm) at the washbasin location with the door partially closed, and the dramatic effect of reorienting the inlet flow can be observed by comparing it with Fig. 6a. The latter is obtained at identical location, but for a fully-open washroom door. The differences are more prominent in the corresponding videos (see multimedia view). The door at 15° directs the incoming fresh air towards the washbasin, which carries the smoke away very effectively towards the exit (to the left). Also, a smaller opening available at the partially-closed door results in a higher inlet velocity, which deflects the smoke streak by a large angle and makes it close to a horizontal direction. This is apparent in Fig. 8b in terms of a large fraction of the time-averaged velocity vectors inclined at more than 80° to the vertical direction. A positive deflection indicates primary flow or well-ventilated region, as observed in "Primary Flow".
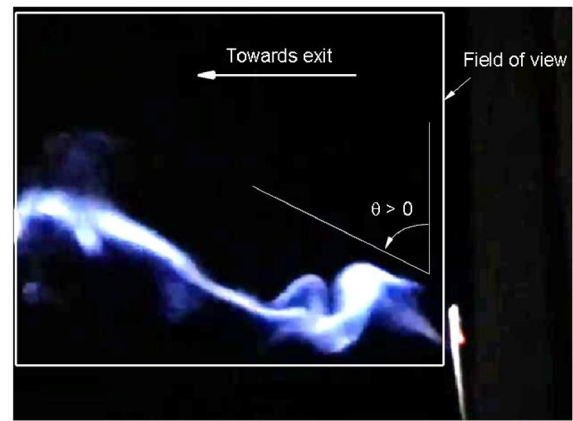
(a)
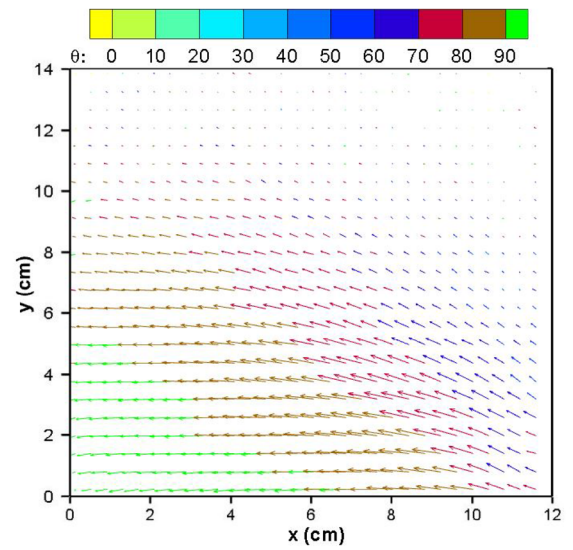
(b)
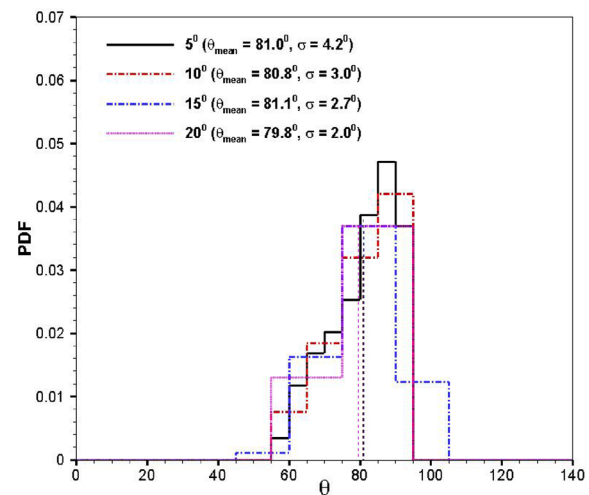
(c)

Figure 8c shows the PDF of the deflection angle computed from the time-averaged velocity vectors. It has a distinct peak in the range $\theta = 80$–$90°$. The average deflection $\theta_{mean} = 81.1°$ and the standard deviation $\sigma = 2.7°$ are obtained, once again, using a velocity filter of 20% and PIV interrogation window (260, 195, 130, 65). This corresponds to (5.7, 4.3, 2.9, 1.4) cm in physical dimensions. The figure shows the variation in the PDF due to changes in the histogram window from 15° (used in the earlier PDFs) to other values (5°, 10° and 20°). All the four PDFs are comparable, and changing the deflection interval has minimal effect on the mean and standard deviation values computed from the PDFs. Similar results are obtained for the other two experiments (presented in "Primary Flow" and "Reversed Flow") and the data are not reported for the sake of brevity. Figure 8a and the corresponding multimedia view show that the smoke forms a discontinuous streak with intermittent regions of vanishing smoke. This could be an effect of the higher air flow velocity. Studying the effect of the velocity magnitude on the smoke streak is left for future studies. For the current purpose, it is important to note that the mean deflection of the smoke streak is close to 80° [see Fig. 8c]. It is positive, i.e. towards the exhaust fan, and hence desirable for evacuating infectious aerosol from the washbasin. Figure 9 compares the PDFs obtained from the three experiments, and clearly shows the potential of the smoke deflection technique to distinguish between primary flow toward the exit and reversed flow in the opposite direction. The PDFs are demarcated by the $\theta = 0$ line, with the primary flow PDFs entirely in the $\theta > 0$ range, while the reversed flow PDF is restricted to the negative θ values. Moreover,

the PDFs for primary flow have a higher peak and a lower spread than the one in the reversed flow. This is indicative of higher unsteady oscillations in the recirculation zone. The highest value of PDF is obtained in the range $75° < \theta < 90°$ for the partially closed door, possibly due to higher air flow velocity in this case. Once again, investigation of the effect of velocity magnitude will be taken up in subsequent studies.

Comparison with CFD

In this section, we present and analyze the CFD solution of an identical washroom geometry, so as to make meaningful comparison with the experimental data. It is important to understand the three-dimensional air flow pattern in the washroom, as obtained from CFD. We, therefore, analyze the CFD solution presented earlier (in "Geometry and Airflow Pattern") in more detail, in terms of the velocity field along multiple planes. The location and orientation of the planes are based on where and how the experiments were conducted. We also look at three-dimensional streamlines to decipher the complex flow pattern in the recirculation zones. This is followed by quantitative comparison with experimental measurements.

The CFD solution is available in terms of the time-averaged steady state velocity field. The fluid is air, and it is assumed to be an ideal gas. In contrast, the smoke from incense sticks consists of combustion gases and soot particles. The particles are in the range of 0.05 to 2.5 micron in size (Jetter et al. 2002; Ji et al. 2010), with a specific gravity of around 1.06 g/cc (Cheng et al. 1995). Particles of this size range are not expected to alter the air flow significantly (Raffel et al. 2018). Further, the effect of gravity on such small particles can be neglected. Thus, they can be expected to follow the local air flow direction, and their path can be compared with the fluid velocity vectors and flow streamlines obtained from CFD. There will, however, be an effect of buoyancy due to a finite difference in temperature between the smoke and the surrounding air, and this is discussed subsequently.

Figure 10 plots the three-dimensional velocity vectors on horizontal planes at $y = 1.2$, 1.0 and 0.6 m. The geometric details of the washbasin and the toilet seat are also included for reference. The pattern is similar to the two-dimensional pattern shown in Fig. 2, in terms of the primary air stream entering through the door and flowing over the toilet seat. The recirculation zone over the washbasin is also visible in part (a) and (b) of the figure. It is marked with smaller velocity vectors than the primary flow. The vector field in part (c) shows the effect of geometric obstructions in the washroom, with small recirculation zones forming next to the washbasin. There is noticeable vertical component of the air flow as it approaches the exhaust fan (on the left wall at a
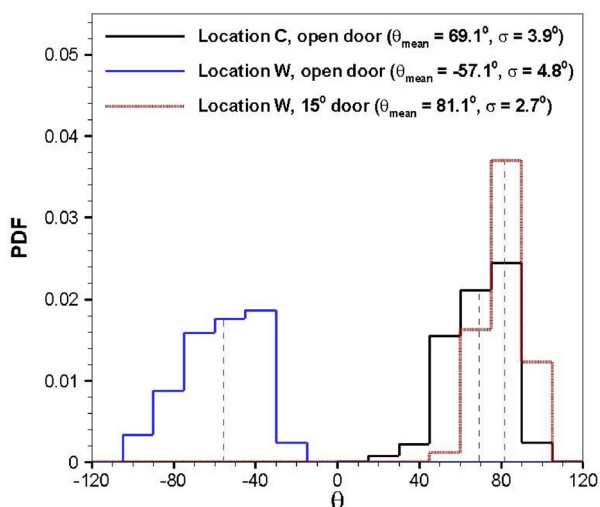

Fig. 9 A comparison of the probability density function of the time-averaged deflection angle obtained from the three experiments, namely, location *C* and location *W* with open door and location *W* with 15° door
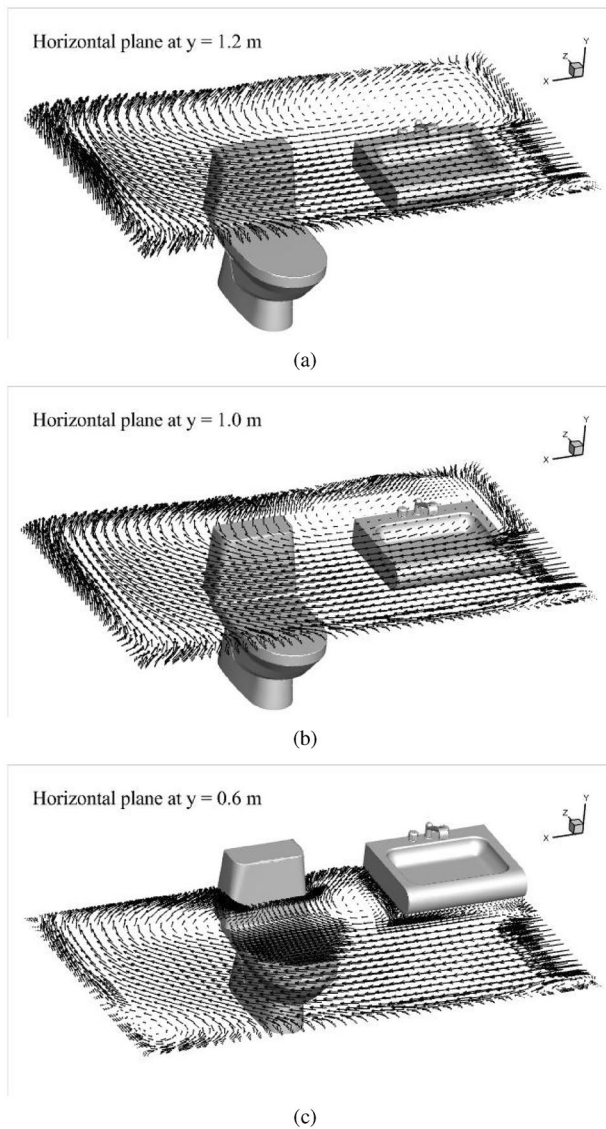
Fig. 10 CFD solution of the air flow pattern in the washroom is presented in terms of velocity vectors plotted in different horizontal planes: **a** $y = 1.2$ m, **b** $y = 1.0$ m and **c** $y = 0.6$ m

Fig. 11 Velocity vectors plotted in **a** a vertical plane at $z = 0.92$ m, with **b** a magnified view of the region over the toilet seat

height of 1.63 m). The three-dimensionality of the velocity field is also prominent along the walls of the washroom, with a significant vertical component.

Location *C* with Open Door

The coordinates of the tip of the incense stick placed at location C is identified as (1.38, 0.61, 0.92), and is marked by ⊗ in Fig. 11. All the dimensions in this section are given in m, unless mentioned otherwise. The figure shows the velocity vectors in a vertical plane at $z = 0.92$ m. This is comparable to the plane in which the smoke visualization is reported in Fig. 4a. Once again, the primary flow from the door (on the right) is characterized by uniform velocity vectors over
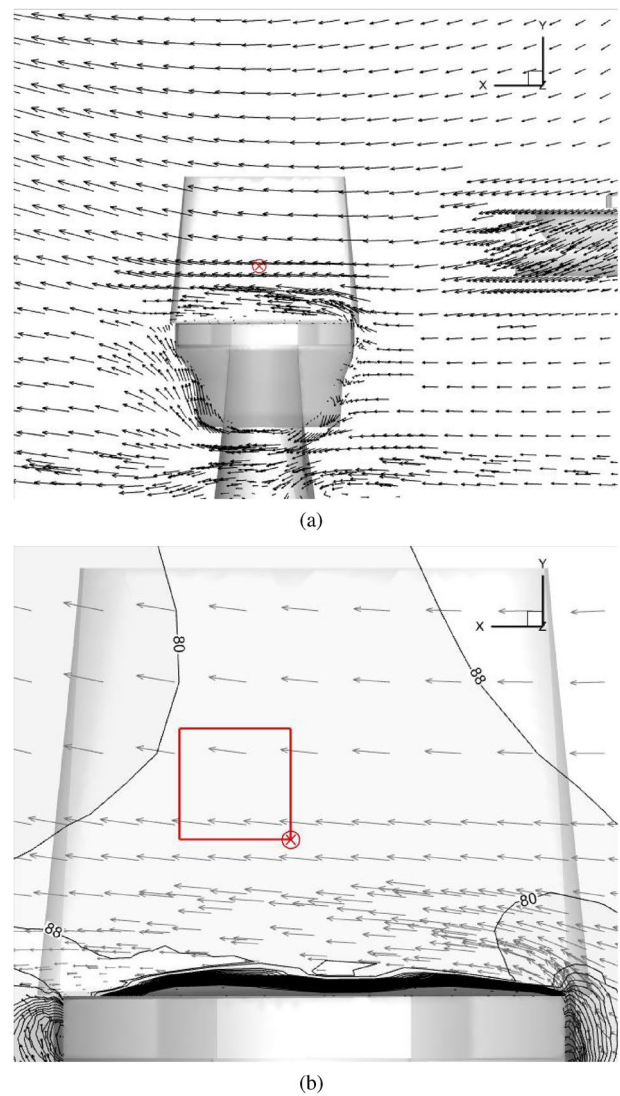
the toilet; it is directed towards the exhaust fan at top left corner of the figure (not part of the frame). Some effect of the obstruction created by the toilet seat and the washbasin are also visible, but they do not seem to affect the flow at the measurement location; see the magnified view in Fig. 11b.

At the point of experimental measurement, the CFD solution gives x and y components of velocity, u and v as 2.74 cm/s and 0.29 cm/s, respectively. They are used to compute the angle of the velocity vector with respect to the vertical direction.

$$\theta = \tan^{-1}(u/v).$$

The CFD solution also provides the velocity component in the z-direction as $w = 1.06$ cm/s. We compute the resultant

horizontal velocity and use it to calculate the deflection from the vertical direction as

$$\theta' = \tan^{-1}(\sqrt{u^2 + w^2}/v).$$

Including the z-component of velocity changes the deflection angle by $\theta' - \theta \simeq 1°$; it does not affect the comparison with experiment significantly, as shown below.

Figure 11b also presents a contour plot of the deflection angle (θ) computed from the CFD solution in the z = 0.92 m plane. It shows that θ is relatively uniform in the region over the toilet seat. Larger variations are limited to the vicinity of the toilet seat and its edges. This is due to the distortion in the primary flow caused by the geometric obstruction. A significant region around the measurement location, including the experimental field of view (red box), has $80° < \theta < 90°$. A quantitative comparison between CFD and experimental deflection values is presented at the end of the section.

Location W with Open Door

We next study the CFD velocity field in a vertical plane at $z = 1.27$ m passing through the washbasin (Fig. 12). The smoke visualization location (0.35, 1.12, 1.27) is marked by ⊗ in the figure.

There are a couple of important differences between the toilet seat and washbasin velocity field. First, the magnitude of velocity is lower by a factor of about seven. This is typical of recirculation zones, which have significantly lower air flow velocity than primary flow. Second, the velocity field in Fig. 12a shows a circulating pattern over the washbasin, in contrast to relatively uniform primary flow over the toilet seat. This translates to a higher variation in the θ values (see the contour plot in Fig. 12a) around the measurement location. Once again, quantitative comparison between CFD and experimental deflection angle is presented at the end of the section.

In fact, the velocity field is quite complex and the full three-dimensional view is presented in part (b) in terms of the streamlines colored by the z-coordinate. The streamlines follow multiple loops as the air circulates over the washbasin and gradually moves towards the ceiling. The streamline loops are such that the reversed flow ($u < 0$) parts are over the washbasin (green and blue color for $1.1 < z < 1.4$), while the forward flow ($u > 0$) is for $z < 1.0$ (orange and red color streamlines). The forward flow is close to the primary flow, where the velocity vectors are pointed towards the exhaust fan. Inside the washbasin, the streamlines are affected by the local geometric features, and have significant vertical component. Nevertheless, the majority of the recirculation zone has negative or reversed velocity as per CFD, and this matches with the negative deflection of the incense smoke (away from the exit location) measured in the experiment.
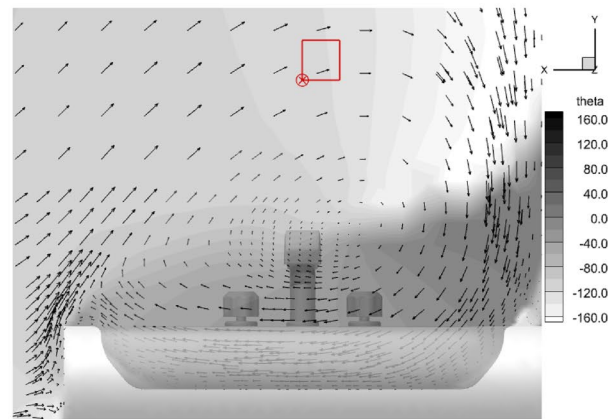
(a)
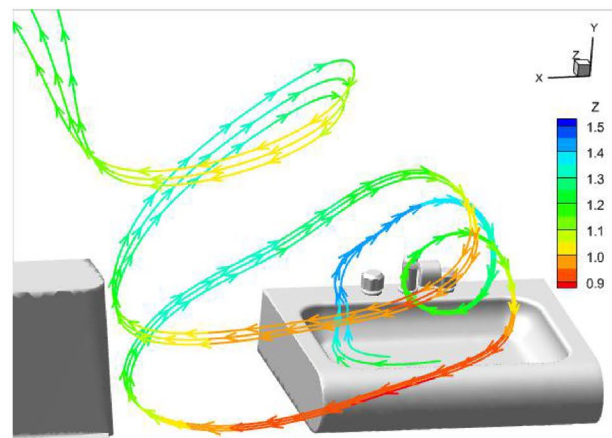
(b)
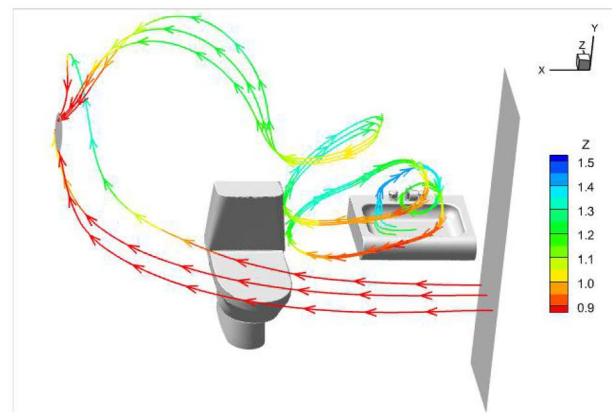
(c)

Fig. 12 Complex three-dimensional air flow circulation over the washbasin is visualized in terms of **a** velocity vectors in a vertical plane at $z = 1.27$ m, **b** streamlines over the washbasin and **c** streamlines in primary and recirculating flow

This is true irrespective of the exact location and height of the incense stick ($y > 1$ m, relevant for human use) in the washbasin, and was observed experimentally (data not included). Overall, the deflection of the smoke streak in the negative direction, when juxtaposed with the positive

deflection in primary flow, is a clear indicator of recirculating air flow over the washbasin.

Figure 12c compares the streamlines in the recirculation zone with those in the primary flow. The red streamlines ($z < 1.0$ m) originate from the door, pass over the toilet seat and exit through the fan (except for a small circulation near the exit location). Thus the air over the toilet seat is replaced by fresh air quickly, and any infectious particles generated in the toilet is evacuated effectively. On the other hand, air in the recirculation zone above the washbasin takes a circuitous route to the exhaust fan. This, along with low velocity magnitude, results in high age of air in this region. The recirculation zone retains infectious particles much longer than the well-ventilated regions covered by the primary flow, as shown in a recent work for identical geometry (Sinha et al. 2021).

Location *W* with Partially Closed Door

CFD simulations were performed with a partially closed door, following a procedure identical to that described in Geometry and Airflow Pattern. The door is deflected at 15° with respect to a fully closed position, and the computational grid is modified appropriately. The door surface is modeled as a no-slip wall and the opening of the door is prescribed as a pressure boundary with zero gauge pressure. Other boundary conditions, including the fan CFM, and grid resolution are maintained as earlier.

Sample CFD results are presented in Fig. 13 in terms of velocity vectors plotted in a horizontal plane at y = 1 m and a vertical plane at z = 1.27 m. The location of the incense tip is marked by ⊗ and the experimental field of view is shown by a red box, as earlier. The dramatic difference compared to the fully open door (Fig. 10) is clearly visible, with the velocity vectors directed into the washbasin corner. The top view in Fig. 13a shows that the fresh air from the door flows over the washbasin, along the wall and towards the exhaust fan. The partially open door creates a uniform primary flow in the vertical plane shown in Fig. 13b, where the velocity vectors are almost horizontal for a majority of the space above the washbasin. CFD predicts $\theta \simeq 90°$ for $y = 0.9$ m to 1.7 m (except near the wall). This covers a large fraction of the space used by a person at the washbasin, and it has primary flow of fresh air from the door.

Thus we are able to ventilate the washbasin area by keeping the door partly closed between two usages of the washroom. It eliminates the recirculation zone completely from the frequently used washbasin location, while creating other recirculation zones behind the door. Further studies are required to evaluate the effect of the new circulation zones on the ventilation of the washroom. Similar strategies of blowing air into a washbasin corner can be achieved by placement of additional fans or by suction/
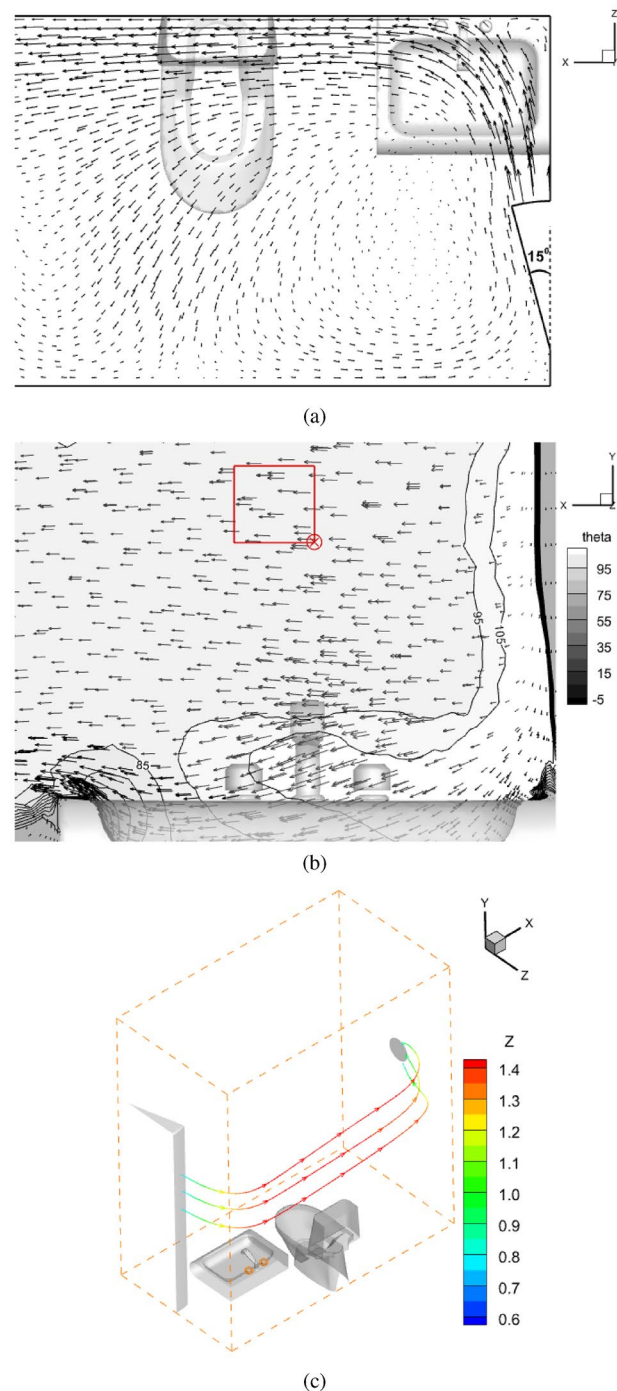

(a)

(b)

(c)

Fig. 13 Velocity vectors plotted in **a** horizontal plane at $y = 1.12$ m, **b** vertical plane at $z = 1.27$ m, computed for the washbasin region with a partially closed door, and **c** showing 3D streamline in primary flow over washbasin

blowing devices. These, however, will have additional power requirement. Deflecting the door or placing louvers, by comparison, is a zero-energy cost retrofit solution for refreshing the air in the frequently-used location of the washbasin.

Quantitative Comparison

Table 2 compares the angle of the velocity vector θ obtained from CFD, with the smoke deflection angle for the three cases reported above. The experimental data are listed in terms of $\theta_{mean} \pm \sigma$ computed from the PIV data over the field of view of the experiment. In a similar vein, the CFD data are taken from a region comparable in size and position (with respected to the tip of the incense stick) in each case. It is found that the CFD deflection angles reproduce the qualitative trend observed in the experimental values. Specifically, the highest deflection is at the washbasin location for the 15° door in both CFD and experiments. This is due to the high inlet velocity through the partially closed door, as discussed above. The lowest magnitude, on the other hand, is seen for the fully open door and the washbasin location, indicative of the low air velocity in the recirculation zone.

In general, the CFD values are higher in magnitude than those obtained from experiments. This could be because of the effect of buoyancy that tends to make the smoke streak more vertical than the air flow velocity in the CFD solution. Additional simulations including the effect of buoyancy are required to address this discrepancy. Nevertheless, the CFD values are comparable to the experimental measurement, within about 8° to 20°. The difference is lower in the primary flow regions, while the highest discrepancy is observed in the recirculation zone over the washbasin for the open door configuration. The variability in the CFD θ values is also considerably high in the latter case, owing to the vortical nature of the velocity field. The variation of the CFD deflection angle ($\pm 5.8°$) for the reversed flow is more than four times larger than that for the primary flow regions ($\pm 1.4°$).

Overall, the experimental measurements match the qualitative trends in the CFD solution. We also get reasonable quantitative comparison between the two sets of data for all the three cases tested in this work. Most important, there is clear corroboration of the positive and negative deflection obtained in primary flow vs. reversed flow. This allows us to experimentally identify the recirculation zone over the washbasin (when the door is open) in a real washroom. The procedure can be extended to identify the extent of the recirculation zone, by carefully mapping the regions of reversed flow and by performing experiments at many more points

over the washbasin. We are also able to experimentally show how directing air flow towards the washbasin can eliminate the recirculating flow in the region. This is the primary objective of the work, i.e. to use incense smoke deflection technique to identify and eliminate recirculation zones in a real indoor environment.

Discussion

The detailed comparison between the numerical and experimental results presented above brings out an interesting point. The CFD data in this case can be used to extrapolate and extend the applicability of the measurement beyond the field of view of the experiment. For example, the contour plot of θ in a plane passing through the experimental location in Fig. 11b shows that the CFD deflection angle changes by less than 10° over the entire toilet seat. The same can be expected for the experimental deflection angle. Thus the positive θ in the experiment, indicating primary flow, can be assumed to be valid over a much larger region than the immediate vicinity of the incense tip. Knowing the extent of the primary flow region is important for the ventilation of the washroom. It is safe to place people and equipment in primary flow.

It is equally important to know the location and extent of recirculation zones in a room; the knowledge can be used in several ways. First, we can avoid placing people and frequently used devices in such regions. This is particularly useful in the scenario of physical distancing, where offices and restaurants are advised to operate at a fraction of their full capacity (Liu et al. 2021; Wu et al. 2021). Second, ventilation system can be operated in a way to have good air flow at the critical locations of a room. For example, there should be adequate air flow in a classroom at the location where the teacher is talking for the majority of the time. Finally, not all desks in a classroom, or every table in a restaurant are occupied. Hence, retrofit solutions like the placement of exhaust fans and air purifiers, can be designed to minimize or even eliminate recirculation zones at the locations occupied by people (Narayanan and Yang 2021; Abuhegazy et al. 2020; Dbouk and Drikakis 2021). It is interesting to note that simply increasing the air flow rate through existing inlet and outlet ports may not eliminate the recirculation zones (Sinha et al. 2021).

The data presented in this work show that the smoke deflection experiment is an effective way to distinguish between recirculation zones and well-ventilated regions in a room. The simple set up of the experiment, along with the easy availability of incense sticks, allows it to be readily deployed in any real scenario under actual operating conditions. Air flow pattern can thus be studied without any geometric simplification and boundary

Table 2 Comparison of the direction of velocity obtained from CFD with the smoke deflection angle (in degrees) measured in experiments

Case	Experimental	CFD
Washbasin location W	-57.1 ± 4.8	-76.2 ± 5.8
Center location C	69.1 ± 3.9	83.0 ± 1.4
Location W with 15° door	81.1 ± 2.7	88.8 ± 0.6

condition assumptions that are inherent in CFD, or laboratory mockup. It is a low-cost alternative to a full-scale PIV experiment that is difficult to perform in the field. PIV gives the velocity field in a two-dimensional plane (Raffel et al. 2018), while the data from the smoke deflection technique are localized close to the point of measurement. Nevertheless, it is a valuable tool to answer an important question in indoor ventilation, namely, where are the recirculation zones that can retain infectious aerosol for a long time? It can be especially useful in situations where one might not have access to sophisticated instrumentation and cannot afford time-consuming CFD simulations.

The washroom geometry studied in this work is relatively small in size, with one inlet (open door) and one exit (exhaust fan) port. It is easy to identify the direction of the primary flow set up between these locations. The reversed flow in opposite direction then identifies the recirculation region. In rooms with multiple inlets and outlet ports, we can extend the procedure by considering the closest entry and exit points. Larger indoor spaces may also have more complex air circulation pattern, with a number of recirculation zones of different sizes. Additional experiments over multiple points will be needed to characterize all such regions. Even then, the frequently used locations in the room would be of primary interest, and we should attempt to minimize or eliminate recirculating or reversed flow at these locations. Once again, the smoke deflection technique is a powerful tool to assess the effectiveness of retrofit solutions to alter the air flow direction at a point.

Conclusions

In this work, we employ smoke visualization experiments to study the ventilation of a real washroom, and distinguish well-ventilated parts of the room from regions of recirculating air flow. Recirculation zones are known to retain infectious aerosol for much longer than the rest of the room. The experiments use readily available incense sticks as smoke generator, and the images are post-processed using PIV software. The resulting velocity field is used to obtain a quantitative measure of the deflection of the smoke streak by the local air flow. A positive deflection is identified as primary flow towards the exit location, while negative deflection due to reversed flow is characteristic of recirculation zones. The experiments are conducted at the frequently-used locations of the toilet seat and the washbasin, and the results are found to compare well with three-dimensional CFD solution of the washroom geometry. A good match between the CFD data and measurement is also found for the case, when the door is deflected to direct fresh air into the recirculation zone.

References

Abuhegazy M, Talaat K, Anderoglu O, Poroseva SV (2020) Numerical investigation of aerosol transport in a classroom with relevance to COVID-19. Phys Fluids 32:103311. https://doi.org/10.1063/5.0029118

ANSYS (2020) Ansys Fluent—CFD software | ANSYS 2020 R2. http://www.ansys.com/products/fluids/ansys-fluent

Bazant MZ, Bush JWM (2021) A guideline to limit indoor airborne transmission of COVID-19. Proc Natl Acad Sci 118:1–12. https://doi.org/10.1073/pnas.2018995118

Bhagat RK, Wykes MSD, Dalziel SB, Linden PF (2020) Effects of ventilation on the indoor spread of COVID-19. J Fluid Mech 903:F-1-18. https://doi.org/10.1017/jfm.2020.720

Bolashikov ZD, Melikov AK, Kierat W, Popiołek Z, Brand M (2012) Exposure of health care workers and occupants to coughed airborne pathogens in a double-bed hospital patient room with overhead mixing ventilation. HVAC R Res 18:602–615. https://doi.org/10.1080/10789669.2012.682692

Cheng Y, Bechtold W, Yu C, Hung I (1995) Incense smoke: characterization and dynamics in indoor environments. Aerosol Sci Technol 23:271–281. https://doi.org/10.1080/02786829508965312

Cho J, Woo K, Kim BS (2019) Improved ventilation system for removal of airborne contamination in airborne infectious isolation rooms. ASHRAE J 61:8–21

Dbouk T, Drikakis D (2021) On airborne virus transmission in elevators and confined spaces. Phys Fluids 33:011905. https://doi.org/10.1063/5.0038180

Eames I, Shoaib D, Klettner C, Taban V (2009) Movement of airborne contaminants in a hospital isolation room. J R Soc Interface 6:S757–S766

He R, Liu W, Elson J, Vogt R, Maranville C, Hong J (2021) Airborne transmission of COVID-19 and mitigation using box fan air cleaners in a poorly ventilated classroom. Phys Fluids 33:057107. https://doi.org/10.1063/5.0050058

Hviid C. A, Petersen S (2016) An methodology for quality control and draught assessment of room ventilation supply using laser light sheets. In: Clima 2016-proceedings of the 12th Rehva World Congress

Jetter JJ, Guo Z, McBrian JA, Flynn MR (2002) Characterization of emissions from burning incense. Sci Total Environ 295:51–67. https://doi.org/10.1016/s0048-9697(02)00043-8

Ji X, Le Bihan O, Ramalho O, Mandin C, D'Anna B, Martinon L, Nicolas M, Bard D, Pairon J-C (2010) Characterization of particles emitted by incense burning in an experimental house. Indoor Air 20:147–158. https://doi.org/10.1111/j.1600-0668.2009.00634.x

Komperda J, Peyvan A, Li D, Kashir B, Yarin AL, Megaridis CM, Mirbod P, Paprotny I, Cooper LF, Rowan S, Stanford C, Mashayek

F (2021) Computer simulation of the SARS-CoV-2 contamination risk in a large dental clinic. Phys Fluids 33:033328. https://doi.org/10.1063/5.0043934

Li YY, Wang JX, Chen X (2020) Can a toilet promote virus transmission? From a fluid dynamics perspective. Phys Fluids 32:065107

Li X, Mak CM, Ma KW, Wong HM (2021) Evaluating flow-field and expelled droplets in the mockup dental clinic during the COVID-19 pandemic. Phys Fluids 33:047111. https://doi.org/10.1063/5.0048848

Liu H, He S, Shen L, Hong J (2021) Simulation-based study of COVID-19 outbreak associated with air-conditioning in a restaurant. Phys Fluids 33:023301. https://doi.org/10.1063/5.0040188

MathWorks Inc. (2021) Matlab version 9.10.0 (r2021a)

Narayanan SR, Yang S (2021) Airborne transmission of virus-laden aerosols inside a music classroom: effects of portable purifiers and aerosol injection rates. Phys Fluids 33:033307. https://doi.org/10.1063/5.0042474

Raffel M, Willert CE, Scarano F, Kähler CJ, Wereley ST, Kompenhans J (2018) Particle image velocimetry: a practical guide. Springer, New York

Shih TH, Liou WW, Shabbir A, Zhu J (1995) A new eddy viscosity model for high Reynolds number turbulent flows. Comput Fluids 24:227–238

Singer BC, Zhao H, Preble CV, Delp WW, Pantelic J, Sohn MD, Kirchstetter TW (2021) Measured influence of overhead HVAC on exposure to airborne contaminants from simulated speaking in a meeting and a classroom. Indoor Air. https://doi.org/10.1111/ina.12917

Sinha K, Yadav MS, Verma U, Murallidharan J, Kumar V (2021) Effect of recirculation zone on the ventilation rate of a public washroom. Phys Fluids 33:10

Strons P, Bailey J. L, Davis J, Grudzinski J, Hlotke J (2016) Development and validation of methodology to model flow in ventilation systems commonly found in nuclear facilities. In: Nuclear Engineering Division, Argonne National Laboratory, Report No. ANL/NE-16/4. https://doi.org/10.2172/1242409

Verma S, Dhanak M, Frankenfield J (2020) Visualizing droplet dispersal for face shields and masks with exhalation valves. Phys Fluids 32:091701. https://doi.org/10.1063/5.0022968

Wang H, Lin M, Chen Y (2014) Performance evaluation of air distribution systems in three different China railway high-speed train cabins using numerical simulation. Build Simul 7:629–638. https://doi.org/10.1007/s12273-014-0168-5

Wang JX, Li YY, Liu XD, Cao X (2020) Virus transmission from urinals. Phys Fluids 32:081703

Wang JX, Cao X, Chen YP (2021) An air distribution optimization of hospital wards for minimizing cross-infection. J Clean Prod 279:123431. https://doi.org/10.1016/j.jclepro.2020.123431

Wu L, Liu X, Yao F, Chen Y (2021) Numerical study of virus transmission through droplets from sneezing in a cafeteria. Phys Fluids 33:023311. https://doi.org/10.1063/5.0040803

Yang W. J (2001) Handbook of flow visualization. CRC Press, Boca Raton

Yin Y, Gupta JK, Zhang X, Liu J, Chen Q (2011) Distributions of respiratory contaminants from a patient with different postures and exhaling modes in a single-bed inpatient room. Build Environ 46:75–81. https://doi.org/10.1016/j.buildenv.2010.07.003

Zhang Z, Han T, Yoo KH, Capecelatro J, Boehman A, Maki K (2021) Disease transmission through expiratory aerosols on an urban bus. Phys Fluids 33:015116. https://doi.org/10.1063/5.0037452